catalysis

Pt L-edge XANES as a probe of Pt clusters

A. L. Ankudinov,[a] J. J. Rehr,[a]* J. J. Low[b] and S. R. Bare[b]

[a]Dept. of Physics, University of Washington, Seattle, WA 98195-1560 USA, and [b]UOP LLC, Des Plaines, IL 60017. E-mail: jjr@phys.washington.edu

The sensitivity of Pt L-edge XANES to local geometric and electronic structure in various Pt_n clusters is investigated using the *ab initio* self-consistent FEFF8 code. Calculations based on FEFF8 are found to be in good agreement with experiment. For pure Pt clusters the XANES can distinguish between 2- and 3-dimensional clusters. Self-consistency is important in determining the variation of XANES with cluster size. The effect of a support is also studied. In $Pt-Cl_x$ clusters the presence of a Cl-Pt bond leads to a "hybridization peak," i.e., a peak in the Cl d-density of states (d-DOS) mixed with Pt d-states. For Pt-H clusters hydrogen addition is well correlated with the growth of a broad shoulder on the white line. This change is attributed largely to AXAFS, i.e., to a corresponding change in the atomic background absorption.

Keywords: Pt L-edge XANES, catalysis, AXAFS, metal clusters,

1. Introduction

Pt $L_{2,3}$-edge XANES has been used as a probe of the electronic state of supported Pt catalysts for many years. The size, shape and morphology of the Pt particles, and the amount and type of adsorbed species on these particles are important physical quantities that directly affect catalyst performance. Controlling the d-electron density of supported metal particles is paramount for metal catalysis since the adsorption or activation of reactants, and hence the overall chemical reactivity, are largely as result of the interaction of the metal d-orbitals with the valence orbitals of the reactants. Given this importance, a correct physical interpretation of the XANES peaks can help to understand, and therefore predict, the resulting catalytic behavior of the metal.

The improved features of FEFF8 (Ankudinov *et al.*, 1998), compared to earlier versions of FEFF, allows us to update, and expand upon prior studies. These include self-consistent (SCF) potentials, a better treatment of relativistic effects, and a more accurate calculation of the edge position and shape. For small Pt clusters, earlier work by Bazin *et al.* (Bazin *et al.*, 1997) was performed using the FEFF7 code, which is not self-consistent, and therefore less accurate near the absorption edge. Thus the present study should yield more reliable results for the intensity of the white line as a function of cluster size, and extends the study to small Pt clusters of different symmetry. The differences between the FEFF8 and FEFF7 calculations, and thus the conclusions that can be drawn, emphasizes the importance of SCF potentials in XANES calculations, especially in absorption edges with strong white lines that are particularly sensitive to the position of the Fermi energy.

In this paper we use theoretical simulations based on FEFF8 to show that XANES can provide considerable insight into the chemistry of small Pt clusters. The results of our calculations are briefly discussed for 1) small Pt clusters of various sizes and shapes, 2) the effect of adsorbed hydrogen on the XANES, and 3) the effect of
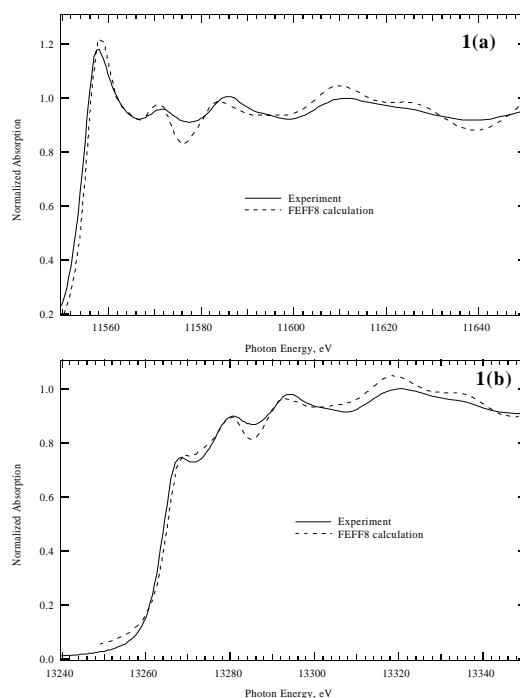
Figure 1
Pt foil XANES. The spin-orbit interaction accounts for the difference between L_3 (Fig. 1a) and L_2 (Fig. 1b) edges. This effect is well reproduced by FEFF8 calculations (dashes), as well as for all peaks in XANES. The experimental data (solid) were recorded at X18B at NSLS using a Si(111) channel cut monochromator in transmission mode, with ion chambers optimized for 20% absorption in I0 and 80% in It.

chloride ligands bonded to Pt. Further details are presented elsewhere (Ankudinov *et al.*, 2000; Ankudinov *et al.*, 2000a; Ankudinov *et al.*, 2000b).

2. Results and Discussion

Relativistic effects are important for heavy atoms like Pt, and hence the spin-orbit interaction must be included to account for the difference between the L_3 and L_2 white line intensity (Fig. 1). The $L_{2,3}$ XANES of Pt foil, as calculated by FEFF8 without a core-hole for a cluster of 87 atoms, is compared to experiment in Fig. 1. Although XAFS calculations are often based on the final state rule, one-particle $L_{2,3}$ calculations for d- and f-elements without a core-hole usually agree better with experiment. A fully screened final state potential with a core-hole may be expected to give worse results, since the screening electron will occupy d or f states, and hence reduce the white line intensity. For single electron calculations this is valid even for d-elements; however, multiplet effects due to the interaction of final d^n configuration with 2p core hole can lead to additional structure. We feel that Fig. 1 demonstrates that FEFF8 without a core hole is adequate for theoretical L-edge XANES simulations for small Pt clusters. Clearly FEFF8 reproduces all spectral features for bulk Pt, including the absence of a
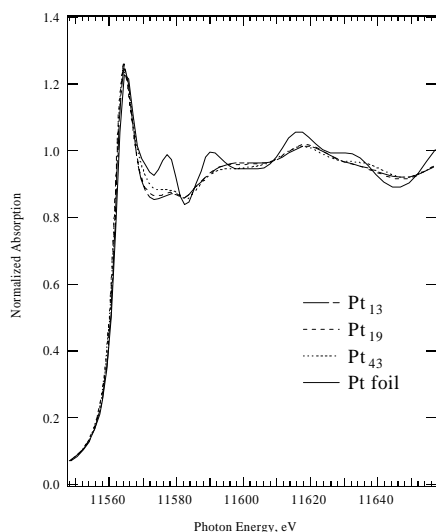
Figure 2
Pt L_3 XANES for spherical clusters of 13 (long dashes), 19 (dashes), and 43 (dots) atoms versus that for Pt foil (solid). Note that the white line intensity is practically invariant, but the peak next to white line may serve as an indication of the cluster size.

Figure 3
Total XANES signal μ decomposed into bare Pt6 absorption (lower curves) and Pt-H bond contributions (upper curves which have been shifted vertically by 1.1) for Pt_6H_2 (solid), and Pt_6H_8 (dash-dots). The difference between these results is due largely to the difference in the atomic background absorption μ_0 for Pt_6H_2 (dashes) and Pt_6H_8 (dots).

white line at the L_2 edge. These results also suggest the need for a dynamic treatment of screening in the x-ray absorption process, since they are at odds with the final state rule. The absence of a white line at the L_2 edge is known to be due to the strong spin-orbit interaction, which favors $j = 5/2$ for the unoccupied 5d electron (Brown *et al.*, 1977, Mattheiss & Dietz, 1980, Mott, 1949). The addition of about 1 eV Lorentzian broadening to account for experimental resolution would make the agreement even better (not shown), but the results shown have no adjustable parameters. The white line intensity is sensitive to self-consistency. Without self-consistency the Fermi level can only be determined to within a few eV by electron gas estimates, and small changes strongly affect the intensity by changing the number of empty final 5d states for dipole allowed transitions.

In a previous study, Bazin *et al.* (Bazin et al. 1997) observed a strong variation of the white line intensity for spherical (cubocta-hedral) Pt clusters with FEFF7 code. A key finding of their work was the realization that different potentials for the different types (coordination) of Pt atoms should be used, and hence the calculated XANES should be a configurational average of these different sites (see Bazin *et al.*,1997, p. 5333). Fig. 2 shows our results from FEFF8 for the same Pt_n clusters (with $n = 13$, 19 and 43), and with the same configurational averaging as used by Bazin *et al.* With the present SCF calculations, the white line intensity now remains approximately constant for the 13, 19 and 43 atom clusters, which is consistent with a fixed Pt 5d charge count, while all the other EXAFS-type features increase in intensity with increasing average coordination number N. Note too that the XANES for the biggest spherical cluster of 43 atoms examined here begins to resemble the bulk spectrum (Fig. 1). These data and those of many other Pt_n clusters, are presented in detail elsewhere (Ankudinov *et al.*, 2000a).

Hydrogen adsorption on small Pt particles causes dramatic changes in the XANES spectra at the Pt $L_{2,3}$-edges. At the Pt L_3-edge the white line intensity decreases and the spectra broaden to
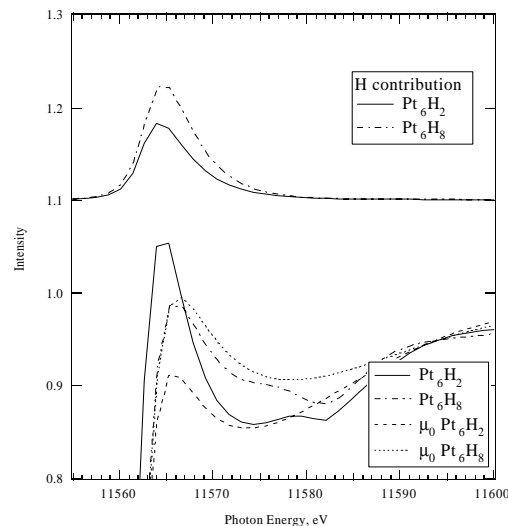
higher energies as hydrogen is added. There have been many efforts to interpret these effects (e.g. Ramaker *et al.*, 1999, Lytle et al., 1985, Samant & Boudart, 1991, Ichikuni & Iwasawa, 1993, Reif-snyder *et al.*, 1997, Watari & Oshnishi, 1997). In particular, in the recent work (Ramaker *et al.*, 1999) an attempt is made to separate the electronic and geometric effects of H adsorption using a novel analysis technique involving experimental peak alignment and theoretical calculations based on the FEFF7 XANES code. They attribute the difference signal to significant Pt-H multiple scattering (MS) between 3-20 eV above the edge. In addition they concluded that a Pt-H antibonding state produces a shape resonance 0-5 eV above the edge. In our work we performed calculations for a cuboc-tahedron of Pt atoms with a Pt-Pt bond length of 2.774 Å. Hydrogen atoms are placed above the centers of the triangular faces at a Pt-H distance of 1.86 Å. Calculations were carried out for clusters with 2, 4, 6, and 8 H atoms on the Pt_6 cluster. Our calculations agree well with experiment: a reduction in the white line intensity, and the growth of the adjacent shoulder (Ankudinov *et al.*, 2000b). To interpret these data we performed a MS analysis (Fig. 3). The XANES signal can be separated unambiguously by changing the cluster radius into contributions from within the Pt_6 cluster alone, and from Pt-H bonds that extend beyond the Pt_6 cluster. These two contributions are shown in Fig. 3. Surprisingly the bare Pt_6 contribution reproduces the experimental trend of white line reduction and shoulder growth. The biggest Pt-H MS contribution comes only from a region within a few eV of the white line, and does not correspond to the region of the spectrum where the intensity is increasing. Moreover, MS theory permits a natural analysis of the XANES signal μ in terms of atomic background absorption μ_0 and MS contributions from the environment χ, though the relation $\mu = \mu_0(1 + \chi)$. These contributions are also illustrated in Fig. 3. Most of the shoulder growth in the XANES due to adsorbed H results from a systematic increase in the atomic background. This clearly shows that the change in XANES is primarily an electronic
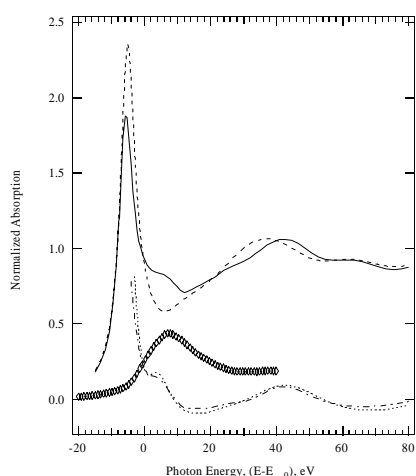
Figure 4
Full calculation for K_2PtCl_6 (solid) and without d-electrons on Cl (dashes). The d-DOS for the Cl atom (diamonds) shows a strong peak at the position of peak B. The XAFS for the first two paths (dots) and for full MS calculations (dash-dot) for the $PtCl_6$ cluster are shown.

effect, due mostly to the effect of the Pt-H bonding potential on the intra-atomic (or embedded atom) potential. This weak intra-atomic scattering has been termed AXAFS (Rehr *et al.*,1994). Remarkably for the Pt_6H_n system the AXAFS is largely concentrated in the XANES. These results are discussed further elsewhere (Ankudinov *et al.*, 2000b).

In the Pt L_3-edge XANES spectra of Pt_xCl_y compounds there is a prominent post-edge peak at about 11575 eV (Ankudinov *et al.*, 2000). We have used FEFF8 to provide some insight to the physical origin of this peak. The results of the calculation are summarized in Fig. 4 for K_2PtCl_6. The post edge peak (peak B in Fig. 4) is interpreted as due to hybridization of the d-photoelectron state with localized Cl-3d states. This assignment is corroborated by parallel density of states (DOS) calculations. The peak in question is roughly coincident with the unoccupied Cl d-DOS. The choice of basis for FEFF8 allows one to include or exclude s-, p-, d-, or f-states for any atom. The disappearance of peak B when Cl d-states are omitted further corroborates connection of the hybridization peak to the unoccupied d-states. In a scattering theoretic description the final d-states reached in the L_3 transition are hybridized with 3d-Cl states primarily through Pt-Cl-Pt and Pt-Cl-Cl-Pt MS paths. Further details are presented elsewhere (Ankudinov *et al.*, 2000).

References

Ankudinov, A.L., Ravel, B., Rehr, J.J. & Conradson, S.D. (1998). *Phys. Rev. B* **5**8, 7565-7576.
Ankudinov, A.L., Rehr, J.J. & Bare, S.R. (2000). *Chem. Phys. Lett.* **3**16, 495-500.
Ankudinov, A.L., Rehr, J.J., Low, J. & Bare, S.R. (2000a). *Submitted for publication.*
Ankudinov, A.L., Rehr, J.J., Low, J. & Bare, S.R. (2000b). *Submitted for publication.*
Bazin, D., Sayers, D., Rehr, J.J. & Mottet, C. (1997). *J. Phys. Chem.* B **1**01, 5332-5336.
Brown, M., Peierls, R.E. & Stern, E.A. (1977). *Phys. Rev. B* **1**5, 738-
Ichikuni, N. & Iwasawa, Y. (1993). *Catal. Lett.* **2**0, 87-95.
Lytle, F.W., Greegor, R.B., Marques, E.C., Biebesheimer, V.A., Sandstrom, D.R., Horsley, J.A., Via, G.H. & Sinfelt, J.H. (1985). *Am. Chem. Soc. Symp. Ser.* **2**88, 280-293.
Mattheiss, L.F. & Dietz, R.E. (1980). *Phys. Rev. B* **2**2, 1663-1676.
Mott, N.F. (1949). *Proc. Phys. Soc. London* 62A, 416-
Ramaker, D.E., Mojet, M.T., Oostenbrink, J.T., Miller, J.T. & Koningsberger, D.C. (1999). *Phys. Chem. Chem. Phys.* **1**, 2293-2302.
Rehr, J.J., Booth, C.H., Bridges, F. & Zabinsky, S.I. (1994). *Phys. Rev. B* **4**9, 12347-12350.
Reifsnyder, S.N., Otten, M.M., Sayers, D. & Lamb, H.H. (1997). *J. Phys. Chem.* **1**01, 4972-4977.
Samant, M.G. & Boudart, M. (1991). *J. Phys. Chem.* **9**5, 4070-4074.
Watari, N. & Oshnishi, S. (1997). *J. Chem. Phys.* **1**06, 7531-7540.